Enhancing Microgrid Resilience and Survivability under Static and Dynamic Islanding Constraints

Agnes M. Nakiganda[1], Shahab Dehghan[1] and Petros Aristidou[2]
[1]*School of Electronic and Electrical Engineering, University of Leeds, Leeds, UK*
[2]*Dept. of Electrical Eng., Computer Eng. & Informatics, Cyprus University of Technology, Cyprus*
el14amn@leeds.ac.uk, s.dehghan@leeds.ac.uk, petros.aristidou@cut.ac.cy

***Abstract*—Microgrids (MGs) are characterised by reduced inertia that can lead to large transients after an islanding event. These transients can result in cascaded device disconnections triggered by protections and consequently to major loss of load or MG blackout. In this paper, a MG operational planning model for grid-connected operation, enhanced with fault-triggered islanding conditions that ensure the MG survivability (both steady-state and dynamic) after islanding is proposed. The dynamic frequency behaviour during islanding using a nonlinear frequency response model is considered by including associated constraints in the planning problem. These include industry limits on the maximum rate of change of frequency, frequency nadir, and the steady-state frequency deviation. The problem is formulated with an iterative multi-stage mixed integer linear model that ensures reliable frequency response, self-sufficiency, and optimal operation of the MG. Simulation results on the CIGRE low-voltage distribution network demonstrate the effectiveness of the proposed model and its suitability in ensuring the reliability, survivability and resilience of a MG.**

***Index Terms*—Microgrid unintentional islanding, frequency response, operational planning, resilience.**

I. Introduction

One of the most important engineering challenges of the century is the design of resilient infrastructure that can survive extreme events and continue to provide services during critical outages. In [1], the resilience of an energy system is said to entail its capacity to tolerate disturbances and continue to deliver affordable energy services to consumers. During reinforcement planning, operators may opt to upgrade existing equipment with more robust designs. In power system operation, however, the solution requires the utilization of control measures that can ensure adaptability, flexibility and fast recovery of power supply to the load demand in the event of a major contingency.

Microgrids (MGs) have been widely proposed as a solution to increase grid resilience to extreme weather conditions and unexpected faults, thus preventing disruptions and system blackouts. In the event of unexpected grid contingencies, MGs can disconnect from the grid and continue supplying local consumers, or at least a critical subset of loads. The successful MG island creation is, however, subject to adequate prior scheduling of the local generation as well as its ability to survive islanding transients.

Different optimisation-based, operational planning (OP) problems with constraints pertaining to the grid-connected and islanded operation have been proposed in literature to ensure self-sufficiency and steady-state security of MGs after islanding events [2]–[5] However, these methods ignore the transients associated with the abrupt grid disconnection in an unintentional islanding event. That is, the proposed methods implicitly assume that the MG will survive the initial voltage and frequency transients and will reach a steady-state equilibrium characterised by the post-islanding power-flow equations. Such formulations provide an optimistic solution concerning the MG survivability. However, violations of security limits during unintentional islanding can trigger different protective devices leading to generator or load disconnections in the MG and the possibility of cascaded failures.

While the variations in power in-feed in a MG affect both the frequency and voltage dynamic security of the network, in this study, we will only focus on the frequency response. The secure dynamic response in OP problems has been addressed in [6]–[8] using heuristic frequency stability constraints, while in [9], [10] linearized analytical frequency related constraints for traditional and low-inertia systems, based on a low-order nonlinear frequency response model [11], are added to the unit commitment models. These studies are however representative of the characteristic behavior of transmission systems and do not reflect the nature of low-voltage (LV) networks.

This paper presents a multi-period, centralised, OP problem for a hybrid MG consisting of a synchronous generator (SG) and converter-interfaced generators (CIGs). The objective is to minimise operational costs and ensure energy sufficiency after an unintentional islanding, with static and dynamic constraints ensuring survivability during and after the event. An iterative solution algorithm of the OP problem that allows to incorporate the non-linear dynamic constraints relating to islanding transients into the OP limits in a tractable manner is proposed. The resilience level of the MG to unexpected disconnection from the main grid is evaluated. Moreover, control measures that can be adopted to improve system flexibility are analysed.

The remainder of this paper is structured as follows. In Section II, we introduce the response model of the MG during and after an islanding event. Section III presents the proposed OP algorithm with the dynamic constraints. In Section IV, we present a case study that analyzes the method's performance. Finally, in Section V, we give some concluding remarks.

II. Microgrid Frequency Response Model

In this section, we present the key aspects of the dynamic behaviour of the MG during the islanding, from which we

The work was supported by the UK Engineering and Physical Sciences Research Council (grant ref. EP/R030243/1).

extract the survivability limits embedded in the OP problem.

The generators of a MG can be either grid-supporting, that is able to provide fast voltage and frequency control during transient events, or units whose active (P) and reactive (Q) power output is only determined by supervisory control and are considered as constant PQ injections during the transients. The transient response and the steady-state operating point subsequent to an islanding incident is governed by the grid-supporting units (SGs and CIGs), in combination with the dynamics of the loads. While this study neglects load dynamics, the methodology can be extended to include their impact.

The frequency response of SGs [11] is governed by the electromechanical dynamics and the turbine governor droop control. In fast-acting CIGs, the active power-frequency droop ensures power sharing and frequency control while inertia response can be emulated by incorporating a virtual synchronous machine (VSM) control loop [12]. Ref. [10] proposes a combined frequency response model incorporating SGs and CIGs with either droop or VSM control. The dynamic metrics governing frequency response in the event of step changes in power in such a network are therein further derived to verify a stable and secure response.

The dynamic frequency response is characterized by the rate of change of frequency (RoCoF) ($\dot{\omega}(t)$) and the frequency nadir/zenith ($\pm\omega_{max}$), while the quasi steady-state (QSS) response is governed by frequency deviation (ω_{ss}). Due to the high penetration of CIGs, the reduced system inertia in MGs can compromise the frequency performance leading to higher nadir/zenith and RoCoF levels. To prevent the activation of under/over frequency protection and RoCoF relays, active power needs to be managed efficiently.

The analytical expressions for the respective characteristics are derived in [10], [12] considering per-unit values as:

$$\dot{\omega}(t) = -\frac{\Delta P}{M} \tag{1}$$

$$\Delta\omega_{max} = -\frac{\Delta P}{D+R_g}\left(1+\sqrt{\frac{T(R_g-F_g)}{M}}e^{-\zeta\omega_n t_m}\right) \tag{2}$$

$$\Delta\omega_{ss} = -\frac{\Delta P}{D+R_g} \tag{3}$$

The aggregated parameters in (1)-(3) and more details on the model derivation are given in [12].

III. Operational Planning Model Formulation with Survivability Constraints

The MG components considered include distributed local generating units (SGs and CIGs) and loads. The loads consist of constant loads as well as flexible loads that can be shifted over time. Linearized *DistFlow* equations [13] are adopted to model power flows in the network.

In the following, N, N_{br}, and T signify the number of nodes, number of branches and the planning horizon, respectively, with t denoting a specific time period. Set $\mathcal{N}$ indexed by $\{i = 1, \dots, N\}$ is composed of the nodes in the MG network, with subsets $\mathcal{N}_{dg}$ and $\mathcal{N}_{pv}$ for nodes with SGs and CIGs, respectively, connected. The branches are contained in set $\mathcal{L}$ denoted by links $\{ij = 1, \dots, N_{br}\}$ where each link (ij) describes the line from node i to node j. Active and reactive power generated and consumed are denoted by p and q respectively. Superscripts "dg", "pv" and "d" represent the power of SGs, CIGs and load respectively. Constant and flexible load is indicated by the superscripts "c" and "f", respectively, to the respective powers. In grid-connected mode, all scheduled load must be satisfied while load shedding is permitted in islanded mode. The power exchanged with the grid at the point of common coupling is denoted as $p_{i=1}^{grid}$ and $q_{i=1}^{grid}$. The system variables include voltage v_i at node i; active/reactive power flows P_{ij}/Q_{ij} between nodes i and j; and net power injection p_i/q_i at a node i, defined as total generation minus load. Finally, r_{ij}/x_{ij} denote the resistance/reactance of the link ij.

A. Solution Algorithm

To ensure both adequacy and survivability of the MG under unintentional islanding, we propose a three-stage solution algorithm where each iteration is indexed by ψ. The proposed algorithm is summarised in the sequel.

First Stage: In this stage, we determine the optimal power schedules for grid-connected and islanded operation models under static constraints, as presented in Sections III-B and III-C, and send the optimal schedules to the second stage.

Second Stage: A disconnection from the main grid will result in a step change of power in-feed to the MG equal to the scheduled grid power exchange at the time of disconnection t, i.e. $\Delta P = p_{ti=1}^{grid}$ in (1)-(3). Thus, the optimal setpoints derived in the first stage for grid-connected operation have to be sufficient to ensure survivability of the MG on islanding *at each hour*, i.e. satisfying the dynamic security limits. In the second stage, we check the OP solution of the first stage against a frequency response model including the system dynamic constraints (1)-(3). The aim of this stage is to ensure that the potential islanding step change of power at each hour t, dictated by the grid power $p_{ti=1}^{grid}$, does not destabilize the MG. Thus, the second-stage problem deals with finding the minimum change (Δp_t^{grid}) on the grid power limits that will ensure the dynamic metrics are not violated, as discussed in Section III-D. The proposed three-stage algorithm stops if the second-stage problem has a zero optimal solution.

Third Stage: A nonzero optimal solution at second stage indicates that the first-stage schedule will not guarantee a secure frequency response at the time of disconnection. In the third stage, we use the nonzero solution of the second stage (Δp_t^{grid}) to tighten limits of power from/to the main grid, updated and applied in the next iteration ($\psi + 1$).

B. Grid-Connected Operation

The model for grid-connected operation is presented in (4) where $u_t^{gc} = [p_t^{grid}, q_t^{grid}, p_{it}^{pv}, q_{it}^{pv}, p_{it}^{dg}, q_{it}^{dg}, p_{it}^{d,f}]$ is the set of control variables.

In the objective function (4a), the first and second terms comprise of the costs attached to active ($C^{grid,p}$) and reactive ($C^{grid,q}$) power respectively exchanged with the main grid.

The import and export costs differ based on the energy market. The third and fourth terms are attached to operational costs (considering negligible start up/shut down costs) of the SGs (C^{pdg}, C^{qdg}) while the fifth term (C^{pv}) is the operational cost of running and maintaining the renewable energy sources. Finally, C^{flex} is a penalty cost incurred when load is shifted away from the customers' preferred consumption periods.

$$\begin{aligned}\min_{u_t^{gc}} \Phi^{gc} = \sum_{t=1}^{T} \Big(C^{grid,p} p_t^{grid} + C^{grid,q} \left| q_t^{grid} \right| \Big) + \\ \sum_{t=1}^{T} \sum_{i \in \mathcal{N}_{dg}} \Big(C_i^{pdg} p_{it}^{dg} + C_i^{qdg} \left| q_{it}^{dg} \right| \Big) + \\ \sum_{t=1}^{T} \sum_{i \in \mathcal{N}_{pv}} C_i^{pv} p_{it}^{pv} + \sum_{t=1}^{T} \sum_{i=1}^{N} C_i^{flex} p_{it}^{d,f}\end{aligned} \tag{4a}$$

s.t.

$$\{P, Q\}_{ijt} = -\{p, q\}_{jt} + \sum_{k:j \to k} \{P, Q\}_{jkt}, \quad \forall t, j \tag{4b}$$

$$v_{it} = v_{jt} - (r_{ij} P_{ijt} + x_{ij} Q_{ijt}), \quad \forall t, (i,j) \in \mathcal{L} \tag{4c}$$

$$p_{it} = p_{t:i=1}^{grid} + p_{it}^{dg} + p_{it}^{pv} - p_{it}^{d}, \quad \forall t,\ i \tag{4d}$$

$$q_{it} = q_{t:i=1}^{grid} + q_{it}^{dg} + q_{it}^{pv} - q_{it}^{d}, \quad \forall t,\ i \tag{4e}$$

$$p_{it}^{d} = p_{it}^{d,c} + p_{it}^{d,f}, \quad q_{it}^{d} = q_{it}^{d,c} + q_{it}^{d,f}, \quad \forall t,\ i \tag{4f}$$

$$-\overline{S}_{ij} \le P_{ij} \pm a_d Q_{ij} \le \overline{S}_{ij}, \quad \forall (i,j) \in \mathcal{L} \tag{4g}$$

$$-\overline{S}_{ij} \le a_d P_{ij} \pm Q_{ij} \le \overline{S}_{ij}, \quad \forall (i,j) \in \mathcal{L} \tag{4h}$$

$$\underline{v}_i \le v_{it} \le \overline{v}_i, \quad \forall t,\ i \tag{4i}$$

$$\{\underline{p}, \underline{q}\}_{t\psi}^{grid} \le \{p, q\}_t^{grid} \le \{\overline{p}, \overline{q}\}_{t\psi}^{grid} \quad \forall t \tag{4j}$$

$$\epsilon_{it}^{pv} \{\underline{p}, \underline{q}\}_{it}^{pv} \le \{p, q\}_{it}^{pv} \le \epsilon_{it}^{pv} \{\overline{p}, \overline{q}\}_{it}^{pv}, \quad \forall t, i \in \mathcal{N}_{pv} \tag{4k}$$

$$\epsilon_{it}^{dg} \{\underline{p}, \underline{q}\}_{i}^{dg} \le \{p, q\}_{it}^{dg} \le \epsilon_{it}^{dg} \{\overline{p}, \overline{q}\}_{i}^{dg}, \quad \forall t, i \in \mathcal{N}_{dg} \tag{4l}$$

$$\{\underline{p}, \underline{q}\}_{i}^{d} \le \{p, q\}_{it}^{d} \le \{\overline{p}, \overline{q}\}_{i}^{d}, \quad \forall t,\ i \tag{4m}$$

$$-r_i^d \le p_{it}^{dg} - p_{i(t-1)}^{dg} \le r_i^u, \quad \forall i \in \mathcal{N}_{dg} \tag{4n}$$

$$\epsilon_{iT_i^{off}}^{dg} - 1 \le \epsilon_{it}^{dg} - \epsilon_{i(t-1)}^{dg} \le \epsilon_{iT_i^{on}}^{dg}, \quad \forall t, i \in \mathcal{N}_{dg} \tag{4o}$$

$$\sum_{t=1}^{T} p_{it}^{dg} \Delta t \le E_i^{dg,p}, \quad \forall i \in \mathcal{N}_{dg}, \tag{4p}$$

$$\sum_{t=1}^{T} p_{it}^{d,f} \Delta t = D_i^p, \quad \forall i \tag{4q}$$

Constraints (4b)-(4c) are the network power flow equations, while (4d)-(4e) relate to the net power injections at each node. The total load, constant and flexible, consumed at each node is given by (4f). Each branch is subject to a maximum loading limit, $\overline{S}_{ij}$, modeled by $P_{ijt}^2 + Q_{ijt}^2 \le \overline{S}_{ij}^2$. This quadratic constraint is linearised by piece-wise approximations constructing a convex polygon [14]. Constraints (4g)-(4h) model the linearised loading limit where $a_d = \sqrt{2} - 1$ is the derivative of the lines constructing the eight segments of the convex polygon. The nodal voltage limits are enforced by (4i) and constraints (4j)-(4m) ensure the limitations on power exchanges from the grid, local generation capacity and total load are not violated. The commitment states of the local generators are indicated by ϵ_{it}^{pv} and ϵ_{it}^{pv}. The active power limits (4j) on grid power are initially (at $\psi = 1$) based on the operator limits, while in the succeeding iterations these are tightened based on the solution to the dynamic response model, as discussed in Section III-D. The SGs are subject to upward (r_i^u) and downward (r_i^d) ramp limits (4n) and minimum on/off times (4o) where parameters T_i^{on} and T_i^{off} define the duration of "on" and "off" periods of the SG, respectively. Energy ($E_i^{dg,p}$) provided by the SG is limited by (4p) within the planning horizon. The total flexible load energy consumption (D_i^p) in an operating cycle is ensured by (4q). The grid-connected operation model in each iteration ψ is a mixed-integer linear programming (MILP) problem.

C. Islanded Operation

The goal in the event of unintentional islanding is to ensure self-sufficiency of the MG. In islanded mode, all loads can be curtailed though critical load is served with priority at all times. The islanded MG self-sufficiency is ensured for at least one time period after disconnection. A robust model considering possible disconnection *at each time period* in the planning horizon is adopted. The problem for islanded operation is formulated as an MILP with the control variables defined by $u_t^{isl} = [\alpha_{it}, \Delta p_{it}^{d,f}, \Delta q_{it}^{d,f}]$. This problem is solved independently for each time period that the MG is potentially disconnected from the grid.

$$\begin{aligned}\Phi_t^{isl} &= \min_{u_t^{isl}} \sum_{i=1}^{N} C_i^{shed,p} \Big((1 - \alpha_{it}) p_{it}^{d,c} + \Delta p_{it}^{d,f} \Big) \\ &+ \sum_{i=1}^{N} C_i^{shed,q} \Big((1 - \alpha_{it}) q_{it}^{d,c} + \Delta q_{it}^{d,f} \Big)\end{aligned} \tag{5}$$

The objective (5) is to minimize load curtailment. The integer α_{it} is "1" when the load on node i is served and "0" otherwise. C_i^{shed} indicates the load priority level and cost of curtailing load at a particular node. The amount of flexible load curtailed is denoted by $\Delta\{p, q\}^{d,f}$. Constraints to system operation are similar to the grid-connected mode with $\{p, q\}_{t:i=1}^{grid} = 0$.

D. Frequency Response Model

Survival of the network i.e. without triggering the operation of protective devices, after an emergency islanding event will depend on the size of the step power change as well as the control capability of the MG generators. The power change is determined by the grid power exchange at the time of disconnection. Given the control parameters and nominal powers of the committed MG units in the grid-connected mode, frequency response can be determined from (1)-(3). The frequency response model is formulated for each iteration ψ and at each time instant as a linear programming (LP) problem (6), solved independently for every time period t.

For each metric, an amount of grid power exchange that will guarantee a secure response at disconnection is determined. To ensure the collective satisfaction of all metrics, a change Δp_t^{grid} in the grid power exchanged at the given time instant

TABLE I
GENERATION UNITS PARAMETERS

	SG	PV1	PV2	PV3	PV4
Node	R1	R11	R15	R17	R18
kW % of peak load	175	350	235	150	90
Inertia (virtual for CIG), H [p.u]	7	7	-	-	-
Damping constant, D [p.u]	25	30	-	-	-
Mechanical power gain, K [p.u]	1.1	1.1	1.1	1.1	-
Droop gain, R [p.u]	0.03	-	0.05	0.05	-
Turbine power fraction, F [p.u]	0.35	-	-	-	-

may be required. The objective (6a), therefore is to determine the minimal change in the grid power schedule at each time instant such that a secure dynamic response is obtained. Constraints (6b)-(6d) define the grid power schedule that will ensure all the operator defined frequency response metric limits indicated by subscript, lim, are satisfied.

$$\Phi_t^{dyn} = \min \quad \left|\Delta p_t^{grid}\right| \tag{6a}$$

s.t.

$$\left|\frac{p_t^{grid} + \Delta p_t^{grid}}{D + R_g} \times \left(1 + \sqrt{\frac{T(R_g - F_g)}{M}} e^{-\zeta\omega_n t_m}\right)\right| \leq \Delta\omega_{max,lim} \tag{6b}$$

$$\left|\frac{p_t^{grid} + \Delta p_t^{grid}}{M}\right| \leq \dot{\omega}_{lim} \tag{6c}$$

$$\left|\frac{p_t^{grid} + \Delta p_t^{grid}}{D + R_g}\right| \leq \Delta\omega_{ss,lim} \tag{6d}$$

A nonzero optimum cost value ($\Phi_t^{dyn} > 0$), indicates that the prior determined schedule for grid-connected operation violates the metric limits. The value of Δp_t^{grid} is utilized to adjust the maximum/minimum limits of power exchanged with the grid in (4j) for the associated time period as indicated in (7). $\overline{\Delta} p^{grid}$/$\underline{\Delta} p^{grid}$ is used to increase/decrease the minimum/maximum limit on power from/to the grid.

$$\underline{p}_{t(\psi+1)}^{grid} = p_{t\psi}^{grid} + \overline{\Delta} p_{t\psi}^{grid}, \quad \overline{p}_{t(\psi+1)}^{grid} = p_{t\psi}^{grid} + \underline{\Delta} p_{t\psi}^{grid} \tag{7}$$
$$\nu\overline{\Delta} p^{grid} + (\nu - 1)\underline{\Delta} p^{grid} = \Delta p_t^{grid}, \quad \nu \in \{0, 1\}$$

IV. CASE STUDY

A modified version of the European configuration CIGRE residential LV network [15] (see Fig. 7.7 in [15]) is used to analyze the performance of the proposed method. The system includes four photovoltaic (PV) generators and one SG. Three of the PV generators have grid-supporting converters while one has fixed output PQ control. The parameters for the MG generators are given in Table I with a system base value of 500 kVA. 50% of the nominal load connected to node R1 is shiftable and nodes R15 and R16 have high priority critical load connected (30% of total load). The load parameters, load profiles and cable parameters are adopted from [15], and typical European generation profiles of the PV units are considered for a 24-hour planning horizon.

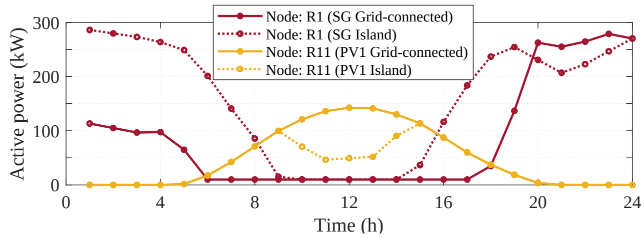

Fig. 1. Power generation of the local MG generators connected at nodes R1 and R11 in grid-connected and islanded modes.

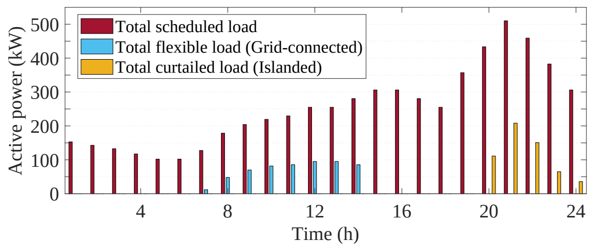

Fig. 2. Network totals of the nominal load profile, shifted load (improving control flexibility) in grid connected mode and curtailed load in islanded mode.

For the dynamic constraints of Stage 2, the ENTSO-E thresholds for frequency nadir at 0.6 Hz, RoCoF at 0.8 Hz/s and quasi-steady-state frequency at 0.2 Hz were used.

The implementation was done in MATLAB R2018b where the optimization model was formulated in YALMIP [16] and Gurobi employed as a solver.

A. Optimal Operation and Adequacy

Fig. 1 shows the power output for each hour in grid-connected and islanded mode for two generators (one SG and one PV, connected to nodes R1 and R11 respectively). In grid-connected operation, the aim is to minimize operational costs while satisfying load demand. As PV units provide free energy, their output is maximized as indicated in Fig. 1.

In islanded operation, the MG should have sufficient generating capacity to serve the critical loads. The sufficiency of the MG is analyzed for each hour in the 24-hour period subject to the PV and SG energy content present at the given hour. As can be observed in Fig. 1, the SG is only utilized in time periods with inadequate solar power to cover the load. Furthermore, in the same figure, the variability of power from PV results in active power curtailment for the PV unit observed during hours 9-14 in islanded mode due to excess PV generation when the MG is islanded. Note that any excess PV power in grid-connected mode is sold to the grid as indicated by the positive values of grid power in Fig. 3 (a).

The variable PV generation and inadequacy of the SG result in load curtailment as indicated in Fig. 2 in some time periods. This is majorly experienced in hours 20 to 24, a part of the peak consumption period (hours 18-24). However, a maximum of 40% load is curtailed in each case, the critical load at nodes remains mostly served in the emergency islanding circumstances. The result provides an indication of the adequacy levels of the MG network showing necessity in better power management of the PV units to improve reliability and better support islanded power modes.

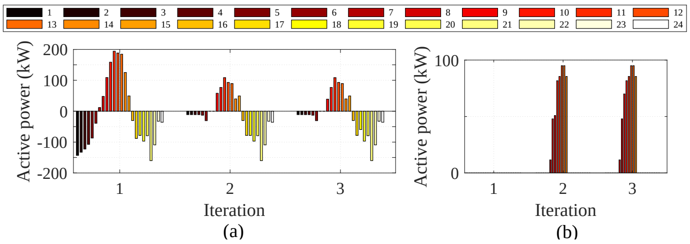

Fig. 3. Variation in (a) power imported (-) from and exported (+) to the grid and (b) flexible load scheduled, as grid power bounds vary at each iteration.

The operational cost in grid-connected mode is minimized by shifting load to the time periods when the system has excess generation from the PV units (hours 7 to 16, Fig. 2). This also minimizes the MG reliance on the grid power and provides more flexibility especially given the limitations that are subject to the power exchange from the grid as shown in Fig. 3.

B. Microgrid Survivability

To minimize performance degradation and prevent cascading faults due to operation of protective relays, the operational schedule is tested to ensure violations of the dynamic constraints are eliminated. The grid power is initially scheduled as indicated by iteration 1 in Fig. 3(a). Iterations 2 and 3 show reductions in the scheduled grid power due to insufficient system control capability to satisfy the dynamic constraints. The variation of RoCoF and QSS frequency metrics depicted in Fig. 4 at each islanding period indicate satisfaction of limits as grid power is reduced at each iteration. The control capability is governed by both the total active power capacity and control parameters of (1)-(3), as defined in Table I. As these parameters are statically defined, further system flexibility is critical. Figure 3(b) shows that the use of flexible loads increased system redundancy preventing infeasibility of the MG model where inadequate power capacity led to unsatisfactory frequency response to meet thresholds. This flexibility is activated in iterations 2 and 3 as a corrective control measure to enhance network survivability during an emergency islanding event.

The level of resilience of a system can be defined by its robustness, redundancy, resourcefulness and rapidity [17]. In this test case, the system robustness and resourcefulness are governed and limited by the control capability of the local generators. The flexible loads in the system are however able to provide the much required flexibility thus improving the overall resilience of the MG in the event of abrupt islanding events. This however comes at an increased cost due to the utilization the costly SG and load-shifting in grid-connected mode to reduce grid power exchange as seen in Fig. 1 and 3.

V. Conclusion

The operational flexibility of power systems is a key attribute in ensuring that the system can survive uncertain and high-impact disturbances. In this paper, we propose a centralized, robust, OP solution that can ensure system survivability as well as self-sufficiency given an abrupt islanding event of the MG. We find that the presence of flexible loads and the control capability of the local generators is vital in improving the MG operational flexibility and robustness. Moreover, we show that not considering the dynamic, transient, behaviour of the MG right after the islanding event, can lead to optimistic solutions and can endanger the survivability of the MG.

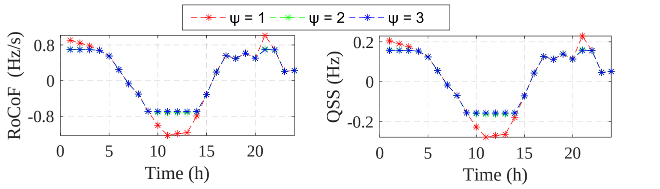

Fig. 4. RoCoF and QSS values at each islanding time instant over each solution iteration. Positive/negative values associated with active power export/import from grid prior to the MG disconnection.

References

[1] M. Chaudry, P. Ekins, K. Ramachandran, A. Shakoor, J. Skea, G. Strbac, X. Wang, and J. Whitaker, "Building a resilient UK energy system," 2009, working paper.

[2] A. Khodaei, "Microgrid optimal scheduling with multi-period islanding constraints," *IEEE Trans. on Power Systems*, vol. 29, no. 3, pp. 1383–1392, May 2014.

[3] C. Gouveia, J. Moreira, C. L. Moreira, and J. A. Peças Lopes, "Coordinating storage and demand response for microgrid emergency operation," *IEEE Trans. on Smart Grid*, vol. 4, no. 4, pp. 1898–1908, Dec 2013.

[4] S. Karagiannopoulos, J. Gallmann, M. G. Vaya, P. Aristidou, and G. Hug, "Active distribution grids offering ancillary services in islanded and grid-connected mode," *IEEE Trans. on Smart Grid*, 2019.

[5] S. A. Arefifar, Y. A. I. Mohamed, and T. H. M. EL-Fouly, "Comprehensive operational planning framework for self-healing control actions in smart distribution grids," *IEEE Trans. on Power Systems*, vol. 28, no. 4, pp. 4192–4200, Nov 2013.

[6] R. Zarate-Minano, T. Van Cutsem, F. Milano, and A. J. Conejo, "Securing transient stability using time-domain simulations within an optimal power flow," *IEEE Trans. on Power Systems*, vol. 25, no. 1, pp. 243–253, Feb 2010.

[7] D. Gan, R. J. Thomas, and R. D. Zimmerman, "Stability-constrained optimal power flow," *IEEE Trans. on Power Systems*, vol. 15, no. 2, pp. 535–540, May 2000.

[8] P. Daly, D. Flynn, and N. Cunniffe, "Inertia considerations within unit commitment and economic dispatch for systems with high non-synchronous penetrations," in *2015 IEEE PowerTech Proc.*, June 2015.

[9] H. Ahmadi and H. Ghasemi, "Security-constrained unit commitment with linearized system frequency limit constraints," *IEEE Trans. on Power Systems*, vol. 29, no. 4, pp. 1536–1545, July 2014.

[10] M. Paturet, U. Markovic, S. Delikaraoglou, E. Vrettos, P. Aristidou, and G. Hug, "Stochastic Unit Commitment in Low-Inertia Grids," *arXiv e-prints*, Apr 2019, arXiv:1904.03030.

[11] P. M. Anderson and M. Mirheydar, "A low-order system frequency response model," *IEEE Trans. on Power Systems*, vol. 5, no. 3, pp. 720–729, Aug 1990.

[12] U. Markovic, Z. Chu, P. Aristidou, and G. Hug, "LQR-based adaptive virtual synchronous machine for power systems with high inverter penetration," *IEEE Trans. on Sustainable Energy*, vol. 10, no. 3, pp. 1501–1512, July 2019.

[13] M. E. Baran and F. F. Wu, "Optimal capacitor placement on radial distribution systems," *IEEE Trans. on Power Delivery*, vol. 4, no. 1, pp. 725–734, Jan 1989.

[14] P. Fortenbacher and T. Demiray, "Linear/quadratic programming-based optimal power flow using linear power flow and absolute loss approximations," *International Journal of Electrical Power & Energy Systems*, vol. 107, pp. 680 – 689, 2019.

[15] K. Strunz, E. Abbasi, R. Fletcher, N. Hatziargyriou, R. Iravani, and G. Joos, "Benchmark systems for network integration of renewable and distributed energy resources," *CIGRE Task Force C6.04.02*, 04 2014.

[16] J. Löfberg, "Yalmip : A toolbox for modeling and optimization in matlab," in *2004 IEEE Intern. Conf. on Robotics and Automation*, 2004.

[17] R. Arghandeh, A. von Meier, L. Mehrmanesh, and L. Mili, "On the definition of cyber-physical resilience in power systems," *Renewable and Sustainable Energy Reviews*, vol. 58, pp. 1060 – 1069, 2016.